



저작자표시-비영리-변경금지 2.0 대한민국

이용자는 아래의 조건을 따르는 경우에 한하여 자유롭게

- 이 저작물을 복제, 배포, 전송, 전시, 공연 및 방송할 수 있습니다.

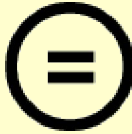
다음과 같은 조건을 따라야 합니다:



저작자표시. 귀하는 원저작자를 표시하여야 합니다.



비영리. 귀하는 이 저작물을 영리 목적으로 이용할 수 없습니다.



변경금지. 귀하는 이 저작물을 개작, 변형 또는 가공할 수 없습니다.

- 귀하는, 이 저작물의 재이용이나 배포의 경우, 이 저작물에 적용된 이용허락조건을 명확하게 나타내어야 합니다.
- 저작권자로부터 별도의 허가를 받으면 이러한 조건들은 적용되지 않습니다.

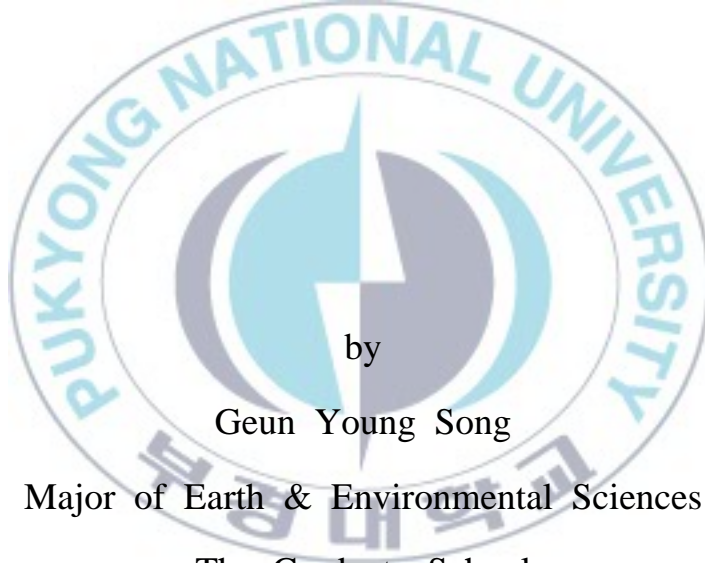
저작권법에 따른 이용자의 권리는 위의 내용에 의하여 영향을 받지 않습니다.

이것은 [이용허락규약\(Legal Code\)](#)을 이해하기 쉽게 요약한 것입니다.

[Disclaimer](#)

Thesis for the Degree of Master of Science

A study of P_n anisotropy beneath continent
in East Asia



Geun Young Song

Major of Earth & Environmental Sciences

The Graduate School

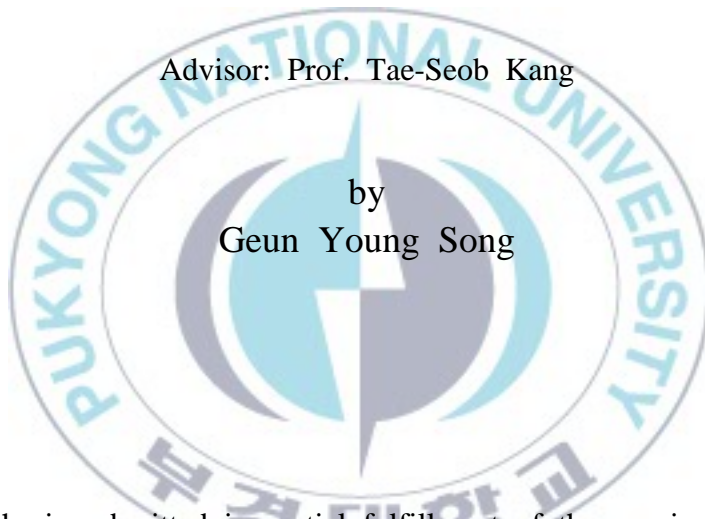
Pukyong National University

February 2014

A study of P_n anisotropy beneath continent in
East Asia

동아시아 지역 P_n 파 이방성 연구

Advisor: Prof. Tae-Seob Kang



by
Geun Young Song

A thesis submitted in partial fulfillment of the requirements
for the degree of

Master of Science

in Major of Earth & Environmental Sciences, The Graduate School,
Pukyong National University

February 2014

A study of P_n anisotropy beneath continent in East Asia

A dissertation
by
Geun-Young Song

Approved by:



(Chairman) Kye-Hun Park



(Member) Young-Seog Kim



(Member) Tae-Seob Kang

February 21, 2014

CONTENTS

Abstract	iii
List of Figures	iv
1. Introduction	1
2. Data	4
3. Method	8
3.1. General model	8
3.2. Inversion	16
4. Results	19
5. Discussion and Conclusion	22
References	24

Appendix	27
Supplemental Table	27
Supplemental Figures	29



A study of P_n anisotropy beneath continent in East Asia

Geun Young Song

Department of Earth & Environmental Sciences, The Graduate School,
Pukyong National University

Abstract

Seismic anisotropy is of importance in elucidating the dynamic processes that occurred in the past and the present within the Earth's interior. If a faster propagation of seismic waves in any azimuth is confirmed, the direction of anisotropy can be estimated beneath the continent. We use P_n waves propagating along the mantle lid to constrain seismic anisotropy in the uppermost part of the upper mantle. We collected P_n arrival times of all events ranging from 1.5° to 15° in epicentral distance in and around East Asia from 1960 to 2011 from the Bulletin of the International Seismological Centre. P_n velocity was estimated using a two-station method to eliminate any unwanted effects of timing error such as the misreading of arrival times from analog seismograms recorded in early instrumental age. Anisotropic regions vary with P_n velocity depending on the azimuth. We created a grid of 1° intervals throughout East Asia. Then seismic anisotropy was identified by the distribution of P_n velocities estimated within a circular spatial window moving on the grid following Smith and Ekström (1999). We then obtained estimates of velocity from each radius cap. Inversion was performed using estimates of data. There are two type of periods which are $\cos(2\varphi)$ and $\cos(4\varphi)$ from inversion. Results may show important points related to plate processes.

List of Figures

- Figure 1. Map of Korean peninsula and Japanese Islands located within East Asia. Korean Peninsula is a stable block connected to The Eurasia Plate. Japan is a relatively active region and mainly younger than 200Ma from the plate margin and the subduction zone. Japan lies at the junction of four major plates: The Eurasian Plate, The Philippine Plate, The Pacific Plate and The North American Plate. 2
- Figure 2. Map of East Asia showing all seismic stations(triangles) and epicenters(circles) that used in this study. 6
- Figure 3. Total travel time versus distance from the source of ISC arrivals. For this region, the travel time curve appears to be linear between 2° and 15° 7
- Figure 4. Two Station Method. A schematic cross section of the two-station method. Using two stations, we obtain estimates of velocity from the differences of travel times identified from collected events. 10

Figure 5. Small opening angle of 4° between the great circle paths of two station pairs and the great circle path of an event to the farthest station. 11

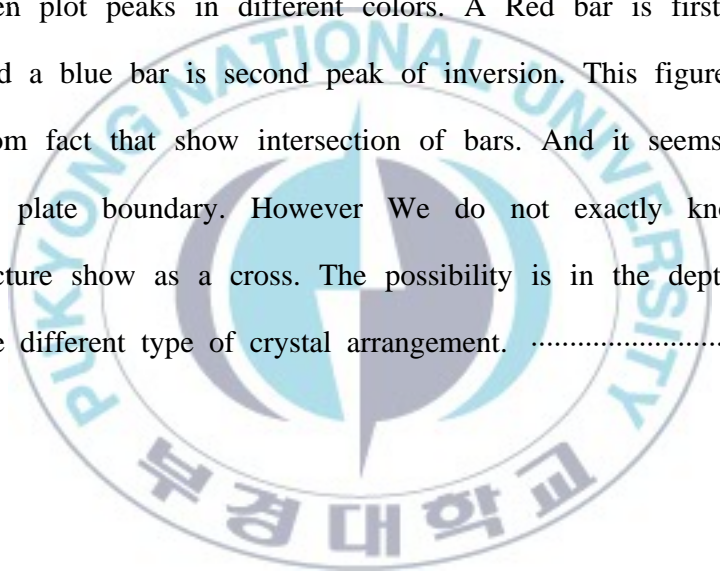
Figure 6. Ray path coverage for the region in East Asia. These paths link pairs of stations with a small opening angles defined as the angle between the great circle paths through the two stations and the great circle path through the event and the farthest station. 12

Figure 7. Velocity is calculated by differences of travel times between station pairs. We use spacing range at least 50km to reduce errors. We only use faster than 7km/s and slower than 8km/s. 13

Figure 8. Velocities of anisotropy with azimuthal variation. The direction of fast P_n anisotropy. 3.0° radius cap is only used for this figure. The direction of anisotropy is spread to the center of the cap. For more information of anisotropy, we may need to compare this with different waves such as SKS of SCS (teleseismic waves). Then we would be more easily able to distinguish them. 15

Figure 9. Results from inversion with estimates of velocity. P_n velocity as a function of an azimuth for a region in East Asia (red dot) and green line represent inversion. Results are 96 estimates of anisotropy from inversion with a 3.0° cap. Small groups of estimates appear depending on the periods of $\cos(2\varphi)$ and $\cos(4\varphi)$ 18

Figure 10. Results of inversion with period 4ϕ . These results have two peak then plot peaks in different colors. A Red bar is first fast velocity and a blue bar is second peak of inversion. This figure is interested from fact that show intersection of bars. And it seems like because of plate boundary. However We do not exactly know why this picture show as a cross. The possibility is in the depth range there are different type of crystal arrangement. 21



1. Introduction

When Earth's material is deformed due to high pressure and temperature, certain types of alignment form. Rays passing through these alignments can have faster or slower velocities. In brief, these features can describe anisotropy. Earth's interior generally consists of anisotropic material, which were identified from seismological studies of anisotropy [Montagner, 1998]. The mantle, a part of Earth interior, is primarily composed of olivine and pyroxene. Olivine is highly anisotropic and this affects the propagation velocity and seismic direction greatly. Anisotropy is typically noticed more in the uppermost mantle. In the lithosphere, seismic anisotropy is generally interpreted as the preferred orientation of olivine and are related to plate tectonic processes [Nicolas and Christensen, 1987; Meighan and Pulliam, 2013]. Accordingly seismic anisotropy is of importance for understanding past and present deformation in the lithosphere [Hearn, 1996; Karato, 1998; Silver, 1996; Stubailo et al., 2012].

The Japanese Islands located within East Asia are highly active regions tectonically. Four major tectonic plates merge in this region: The Eurasian Continental Plate, The North American plate, The Pacific plate and The Philippine Sea Plate(Figure 1). The basement rocks of the

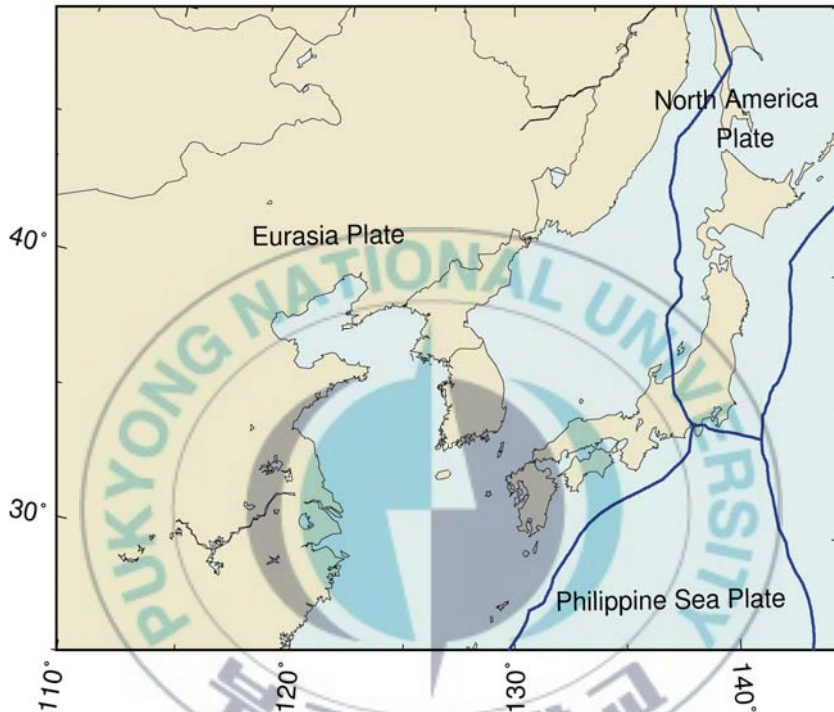


Figure 1. Map of Korean peninsula and Japanese Islands located within East Asia. Korean Peninsula is a stable block connected to The Eurasia Plate. Japan is a relatively active region and mainly younger than 200Ma from the plate margin and the subduction zone. Japan lies at the junction of four major plates: The Eurasian Plate, The Philippine Plate, The Pacific Plate and The North American Plate.

Japanese Islands are composed of young rocks, mainly younger than 200Ma. In Japan thousands of islands are arranged in several arcs and also contain volcanic islands arcs which cover a distance of 3,000km. Ocean Plates subduct at a number of trenches and trough: The Kuril Trench, The Japan Trench, The Izu-Bonin Trench, The Nankai Trough and The Ryukyu Trench. The Korean Peninsula is a stable block that is connected to The Eurasian Plate. The basement layers are mostly formed before the Paleozoic. It is well-known that the geological structure of Korea is relatively more stable than Japan.

In this paper, we use P_n -wave, the first arrival head wave to reach the station passing through the uppermost mantle. P_n -wave velocity which carries information about the uppermost mantle is changes depending on mineral arrangement. Using the difference of velocity, we can identify P_n anisotropy and we then present reasons for these P_n anisotropy beneath the continents in the study area. Inversion is used to compare the relationships between velocity data and calculated data.

2. DATA

We collected P arrival times of all events in East Asia from the Bulletin of the International Seismological Centre (ISC) from 1960 to 2011 (figure 2, 20° to 50° latitude, 110° to 150° longitude). ISC contains locations from 1960 to present all around the world. Because P_n which is the first arrival of P waves possesses information of the upper mantle by traveling beneath the Moho with the uppermost mantle velocity, we then extracted P_n arrival times from the collected data. Arrival times from the stations and event times are already calculated at collected data. We then obtained the velocities from recorded time and location in the study area and the calculated velocities were used to acquire P_n anisotropy in study area.

The determined range from the recorded data can contain not only information of the uppermost mantle but from deeper depths also, thus the range should be decided as follows. The specific range of depths is designated by the relationships between travel time and distance. We only want to collect data from uppermost mantle, however 15° of curvature may pass through deeper depths such as the asthenosphere and figure 3 shows a visible linear relationship from the aforementioned range. Approximately beyond 12°, triplication is observed. Thus we only

use data from the most conservative range of 2° to 12° in and around East Asia. Within this distance range, we can expect to obtain data that is not sampling from the deeper mantle. Previous research also set a range limit below ~16° [Beghoul and Barazangi, 1989; Hearn et al., 1991; Hearn, 1996; Smith and Ekström, 1999; Xing and Ping, 2009].



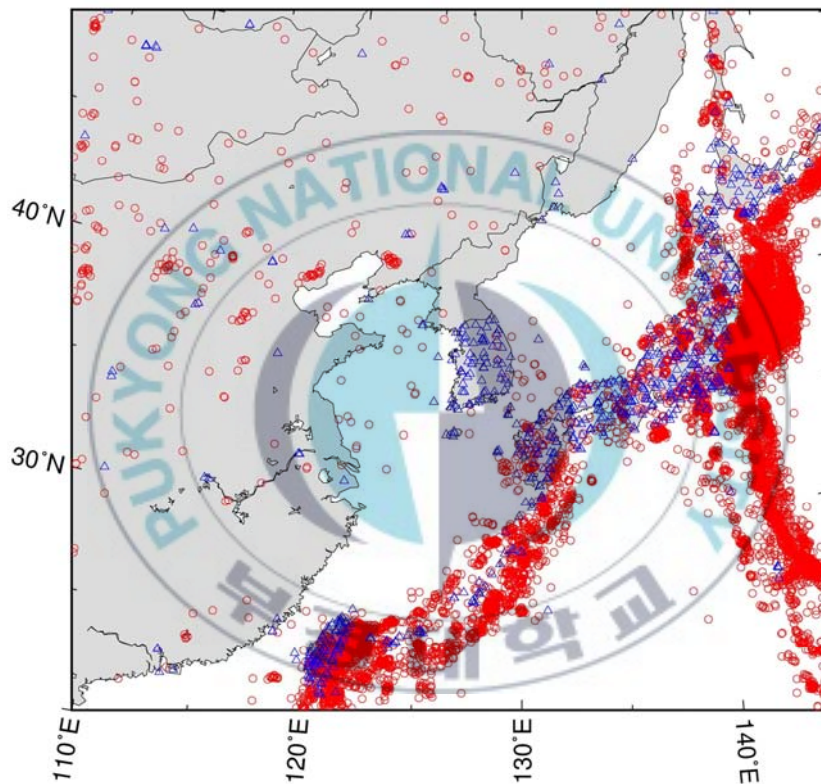


Figure 2. Map of East Asia showing all seismic stations(triangles) and epicenters(circles) that used in this study.

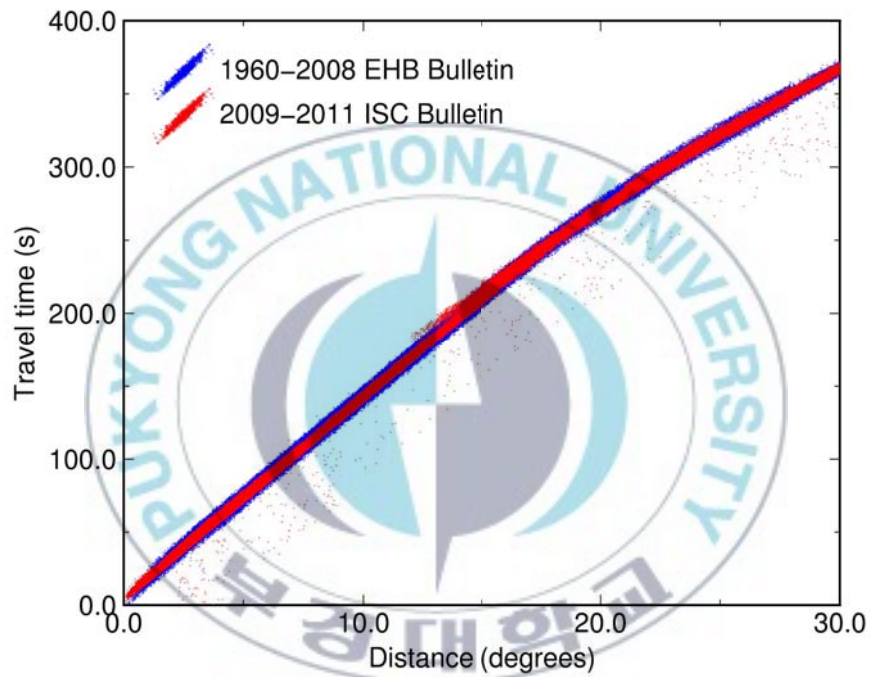


Figure 3. Total travel time versus distance from the source of ISC arrivals. For this region, the travel time curve appears to be linear between 2° and 15° .

3. Method

3.1. General Model

A general model which explains P_n velocity with azimuthal variations indicates weak anisotropy of mantle material. In slight anisotropic medium such as the Earth, dependence for varying azimuth can be described as follows:

$$\alpha(\phi) = \alpha_0 + C\cos(2\phi) + D\sin(2\phi) \quad (1)$$

$$\alpha(\phi) = \alpha_0 + C\cos(2\phi) + D\sin(\phi) + E\cos(4\phi) + F\sin(4\phi) \quad (2)$$

Equation(1) which is simplified from the version of equation(2). Commonly, in studies of anisotropy, mostly equation(1) is used for anisotropic studies in Earth material. However we utilize equation(2) for this study and results of inversion can be explained by the reason we adapt equation(2) rather than equation(1), a general model of anisotropy.

Equation(2) indicates; α_0 is P_n velocity at azimuth ϕ and α_0 is an average P_n velocity in the medium such as within the uppermost mantle [Vetter and Minister, 1981; Smith and Ekström, 1999]. To obtain α_0 , C,

D, E and F, we calculate estimates of velocity from travel times respectively. We apply the two-station method (figure 4). Differences in travel time from the two station pairs is attained by the two-station method but a large error from this method is possible because of overly close station pairs. Thus the first constraint is a minimum station spacing of 50km to reduce errors.

The first restriction of our data is defined as an angular value between the great circle path through two station pairs and the great circle path through the event and the farthest station [Smith and Ekström, 1999]. The opening angle between two great circle paths is restricted to only 4° , within this angular value almost straight lines are made between the two great circle paths (Figure 5, 6). Figure 6 indicates the great circle path which satisfies the restrictions such as opening angle for all stations and events. Taiwan and Japan show more useful coverage for obtaining velocities of anisotropy than China within study area. We make grids with spacing of 1° throughout East Asia to measure estimates of velocity. We use secondary constraints of estimates of velocity; velocities slower than 7.0km/s and faster than 8.0km/s we eliminate for anisotropy in study area, because locations from all events is already calculated by an average velocity model from the ISC catalog, thus there is uncertainty in the estimates (Figure 7). For this reason, uncertainty models show estimates of velocities within the ranges that could contain velocities passing through deeper or shallower depths.

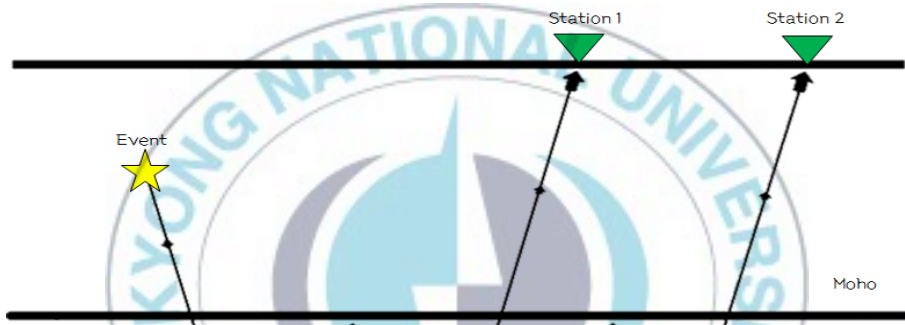


Figure 4. Two Station Method. A schematic cross section of the two-station method. Using two stations, we obtain estimates of velocity from the differences of travel times identified from collected events.



Figure 5. Small opening angle of 4° between the great circle paths of two station pairs and the great circle path of an event to the farthest station.

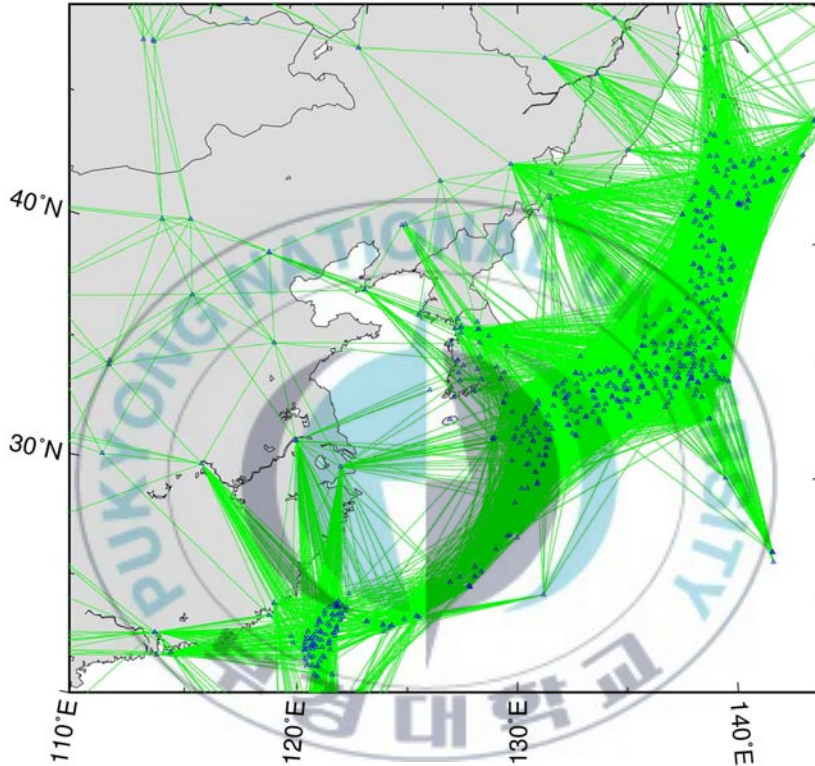


Figure 6. Ray path coverage for the region in East Asia. These paths link pairs of stations with a small opening angles defined as the angle between the great circle paths through the two stations and the great circle path through the event and the farthest station.

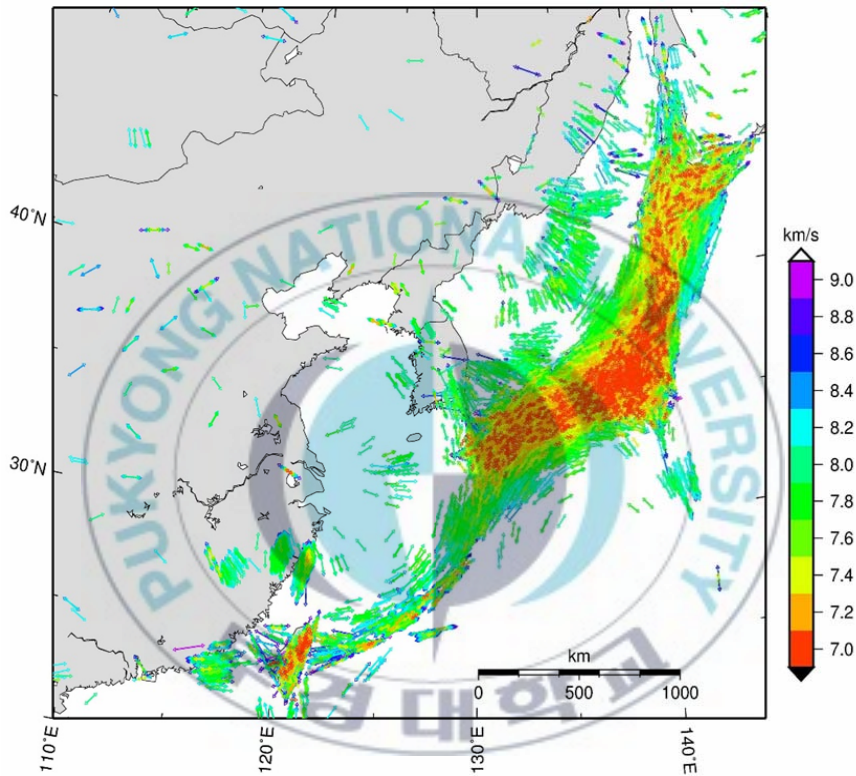


Figure 7. Velocity is calculated by differences of travel times between station pairs. We use spacing range at least 50km to reduce errors. We only use faster than 7km/s and slower than 8km/s.

than the uppermost mantle. To reduce errors from each location, Radius 1.5° cap within the grid are used to identify the direction of anisotropy in the center of the cap (figure 8) [Smith and Ekström, 1999]. Results from the two-station method and the restricted opening angles are presented in Figure 8. As we previously mentioned, the range of distances for station pairs and restricted velocities are used to obtain reliable data thus we are able to trust estimates of velocity if they lie within these strictly constrained conditions.



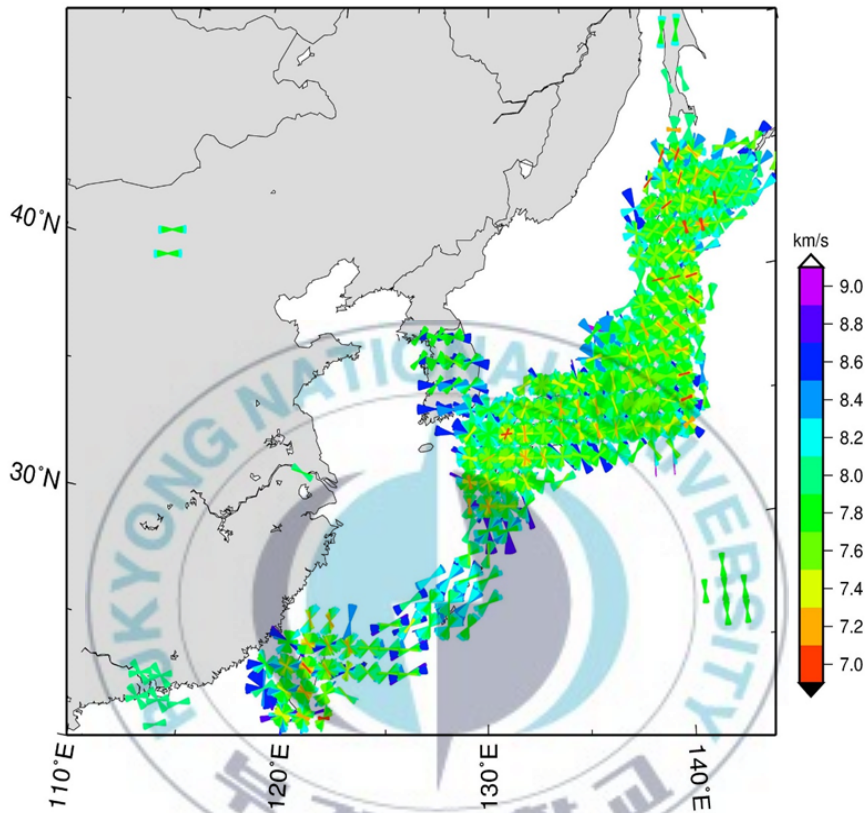


Figure 8. Velocities of anisotropy with azimuthal variation. The direction of fast P_n anisotropy. 3.0° radius cap is only used for this figure. The direction of anisotropy is spread to the center of the cap. For more information of anisotropy, we may need to compare this with different waves such as SKS or SCS (teleseismic waves). Then we would be more easily able to distinguish them.

3.2. Inversion

To convert the data, we apply explicit equations to represent a linear case:

$$\text{Data: } \mathbf{d} = [d_1, d_2, d_3, \dots, d_N]^T$$

$$\text{Model parameter: } \mathbf{m} = [m_1, m_2, m_3, \dots, m_M]$$

$$\mathbf{d} = \mathbf{Gm} \quad [1]$$

where \mathbf{d} is an N-dimensional data vector, \mathbf{m} is an M-dimensional model parameter vector, and \mathbf{G} is an N x M matrix containing only constant coefficients.

We performed inversion using the above formula[1] with equation (1). First, we defined a data vector where:

$$\mathbf{d} = [d_1, d_2, d_3, \dots, d_{360}]^T$$

We applied P_n velocity as a function of the azimuth for the region in East Asia. We only use data from 3.0° cap. To construct following matrix G:

$$\mathbf{G} = \begin{bmatrix} 1 & \cos(2*0) & \sin(2*0) & \cos(4*0) & \sin(4*0) \\ 1 & \cos(2*1) & \sin(2*1) & \cos(4*1) & \sin(4*1) \\ \vdots & \vdots & \vdots & \vdots & \vdots \\ 1 & \cos(2*180) & \sin(2*180) & \cos(4*180) & \sin(4*180) \end{bmatrix}$$

We define model parameter \mathbf{m} using data, \mathbf{d} and matrix, \mathbf{G} ,

$$\mathbf{Gm} = \mathbf{d}$$

$$\mathbf{G}^T \mathbf{Gm} = \mathbf{G}^T \mathbf{d}$$

$$(\mathbf{G}^T \mathbf{G})^{-1} (\mathbf{G}^T \mathbf{G}) \mathbf{m} = (\mathbf{G}^T \mathbf{G})^{-1} \mathbf{G}^T \mathbf{d}$$

And

$$\mathbf{m} = (\mathbf{G}^T \mathbf{G})^{-1} \mathbf{G}^T \mathbf{d}$$



then data, model parameter and matrix are defined using octave (software for numerical analysis) for the inversion of the P_n velocity from our results. Data from inversion and P_n velocities from our results are denoted for interpretation of intrinsic anisotropy that are able to explain the variation in velocities shown in Figure 9. Results of the inversion are possible to identify in the Appendix for the East Asia region.

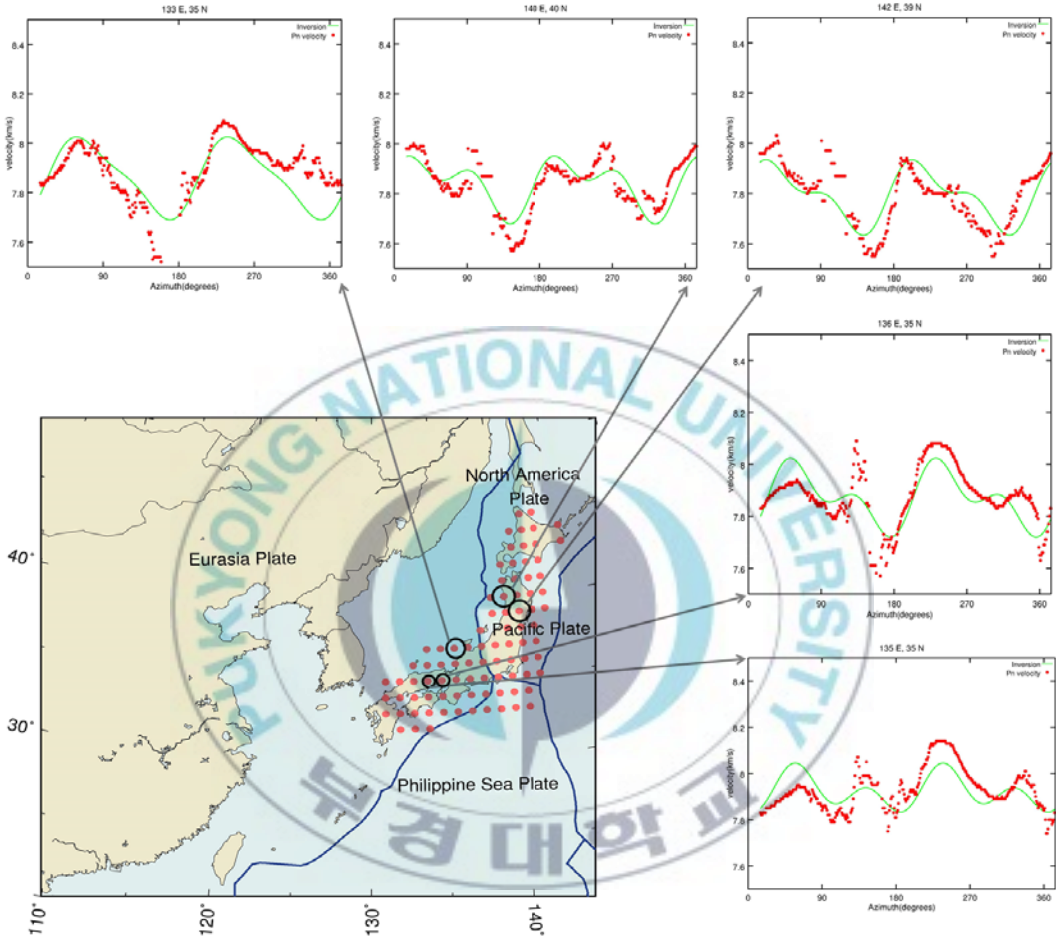


Figure 9. Results from inversion with estimates of velocity. P_n velocity as a function of an azimuth for a region in East Asia (red dot) and green line represent inversion. Results are 96 estimates of anisotropy from inversion with a 3.0° cap. Small groups of estimates appear depending on the period of $\cos(2\varphi)$ and $\cos(4\varphi)$.

4. Results

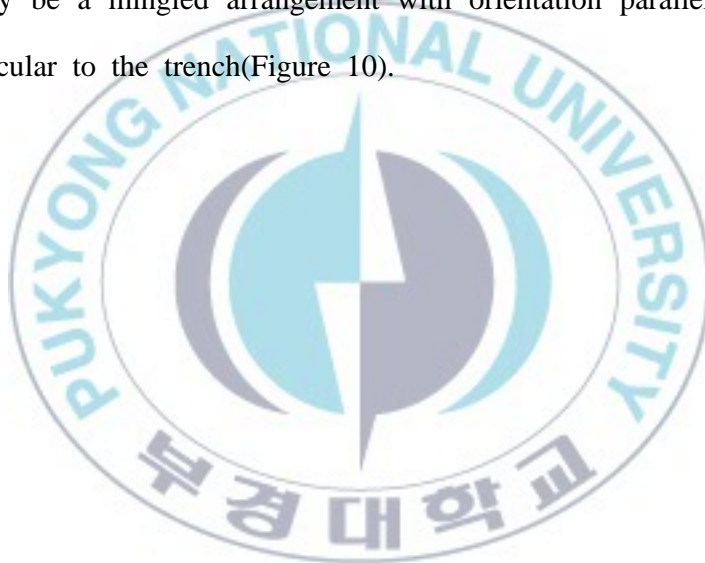
We have obtained 96 estimates of anisotropy are using only a 3.0° cap. Before classifying estimates into quality A and B, we assorted small groups of estimates depending on period of a small $\cos(4\phi)$ signature. Inversion with folded data from our results has mostly $\cos(2\phi)$ signature associated with anisotropy which are simplified to a version of equation(1) to equation(2) [Smith and Ekström, 1999; Buehler et al., 2010].

$$\alpha(\phi) = \alpha_0 + C\cos(2\phi) + D\sin(2\phi) + E\cos(4\phi) + F\sin(4\phi) \quad (2)$$

$$d = Gm \quad [1]$$

However our results from East Asia rarely present different types of signature such as $\cos(4\phi)$ which is a 90° period. Therefore it is necessary to reorganize for inversion with the folded data. Inversion data from our results appear mainly in the region of Japan and then we should therefore consider which part of Japan has produced this data(formula [1]). The mantle wedge of the subduction zone is the location where seismic anisotropy is ordinarily observed; Polarization of the direction of fast transverse wave is parallel to the trench, it generally appears at the forearc of subduction zone. Because of these early

studies of subduction, inversion from short periods such as $\cos(4\varphi)$ can possibly lie away from the subduction zone. Figure 8 has certain directions of anisotropy in Taiwan, two directions are indicated; trench perpendicular and parallel to the boundary of Philippine Plate. Inversion from our data exposes $\cos(4\varphi)$ from several areas which are related to the anisotropy of figure 9. Also some inversion data is generated near The Philippine Plate, we can also consider that this location is close to the trench and boundary of The Pacific Plate, thus inversion may be a mingled arrangement with orientation parallel to the trench and perpendicular to the trench(Figure 10).



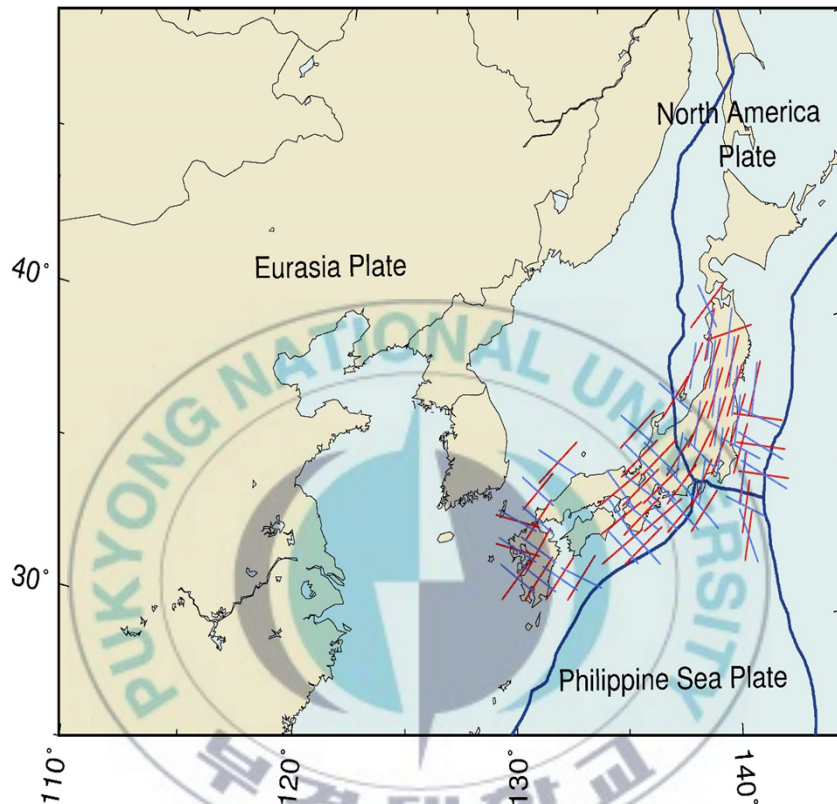


Figure 10. Results of inversion with period 4ϕ . These results have two peak then plot peaks in different colors. A Red bar is first fast velocity and a blue bar is second peak of inversion. This figure is interested from fact that show intersection of bars. And it seems like because of plate boundary. However We do not exactly know why this picture show as a cross. The possibility is in the depth range there are different type of crystal arrangement.

5. Discussion and Conclusion

We found evidence for anisotropy from using the two-station method. East Asia, especially Japan and Taiwan encounter plates such as The Philippine Plate and The Pacific Plate. The collected data have mainly good coverage of nearby Japan because the station range is good enough. We then can consider the data near Japan to be trustworthy. Inversion and estimates of velocity indicate similar results such as the following. Firstly, inversion shows a special period near Japan, $\cos(4\varphi)$. Secondly, estimates of velocity appear in certain directions along the trench. The first means that generally anisotropy can explain the $\cos(2\varphi)$ signature but the data from caps has different periods than normal anisotropy results. Then we should consider an additional way such as including $\cos(4\varphi)$ within the equation. It is possible to interpret that there are mixed anisotropy. For that reason, data for our results and inversion show very short periods. Estimates of velocity support the above explanation.

However the problem is that data from the western part of Japan is not enough to establish our conclusion. Also, the quality of data from a 3.0° cap is not sufficient and the data from 1.5° cap particularly is missing parts. We also need a comparison target to accurately identify a layer of anisotropy, thus SKS splitting may be needed for comparison not only using P_n velocity of East Asia would be better to establish a higher reliability of our results. Therefore we

carefully mention the mixed results near the subduction zone from P_n velocities with inversion from our results, it may possible to mix two type of fast and slow directions.



References

Beghoul, N., and Barazangi M. (1989), Mapping High Pn velocity Beneath the Colorado Plateau Constrains Uplift Models, *Journal of Geophysical Research*, Vol. 94, No. B6, 7083-7104.

Buehler J. S., and Shearer P. N. (2010), Pn tomography of the western United States using USArray, *Journal of Geophysical Research*, Vol. 115, B09315, doi:10.1029/2009JB006874.

CUI Z. X., and PEI S. P. (2009), Study on Pn velocity and anisotropy in the uppermost mantle of the Eastern Himalayan Syntaxis and surrounding regions, *Chinese Journal of Geophysics* Vol.52, 943-952.

Hearn, T. M. (1996), Anisotropic Pn tomography in the western United States, *Journal of Geophysical Research*, VOL. 101, NO. B4, 8403-8414.

Hearn, T., Beghoul, N., and Barazangi M. (1991), Tomography of the Western United States From Regional Arrival Times, *Journal of Geophysical Research*, Vol. 96, No. B10, 16,369-16,381.

Karato, S. (1998), Seismic anisotropy in the deep mantle, boundary layers, and the geometry of mantle convection, *Pure Appl. Geophys.*, 151, 565-587.

Meighan, H. R., and Pulliam, J. (2013), Seismic anisotropy beneath the northeastern Caribbean: implications for the subducting North American lithosphere, *Bull. Soc. géol. France*, t. 184, no 1-2, pp. 67-76.

Montegner, J. P. (1998), Where can seismic anisotropy be detected in the Earth's mantle? In *Boundary Layers... Pure appl. geophys.*, 151, 223-256.

Nicolas, A., and Christensen, N. I. (1987), Formation of anisotropy in upper mantle peridotites: A review. In *Composition, Structure and Dynamics of the Lithosphere-Asthenosphere System*(eds K. Fuchs, and C Froidevaux) American Geophysical Union, Washington, D.C. 111-123.

Sliver, P. G. (1996), Seismic anisotropy beneath the continents: Probing the depths of geology, *Annu. Rev. Earth Planer. Sci.*, 24, 385-432.

Smith, G. P., and Ekström (1999), A global study of Pn anisotropy beneath continents, *Journal of Geophysical Research*, Vol. 104, No B1, 963-980.

Stubailo, T., Beghein, C., and Davis, P. M. (2012), Structure and anisotropy of the Mexico subduction zone based on Rayleigh-wave analysis and implications

for the geometry of the Trans-Mexican Volcanic Belt, Journal of Geophysical Research, Vol. 117, doi; 10.1029/2011JB008631.

Vetter U., and Minster J. B. (1981), Pn anisotropy on southern California, Bulletin of the Seismological Society of America, Vol. 71, No. 5 1511-1530.

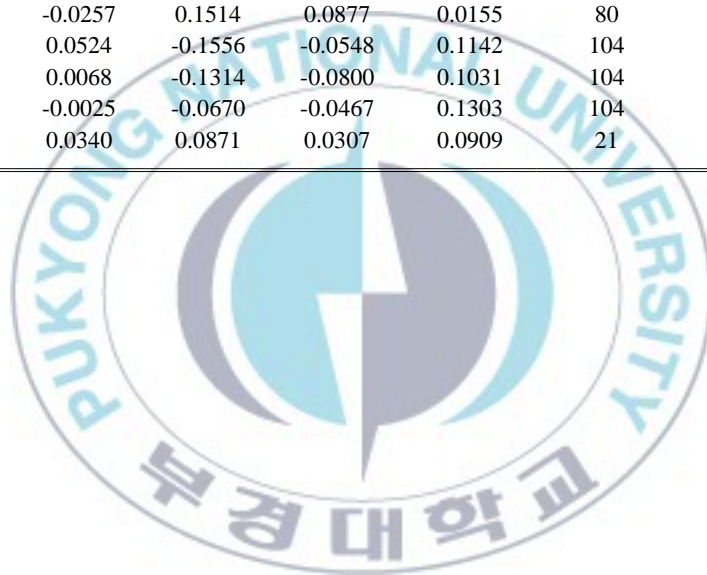


Appendix

Supplemental Table

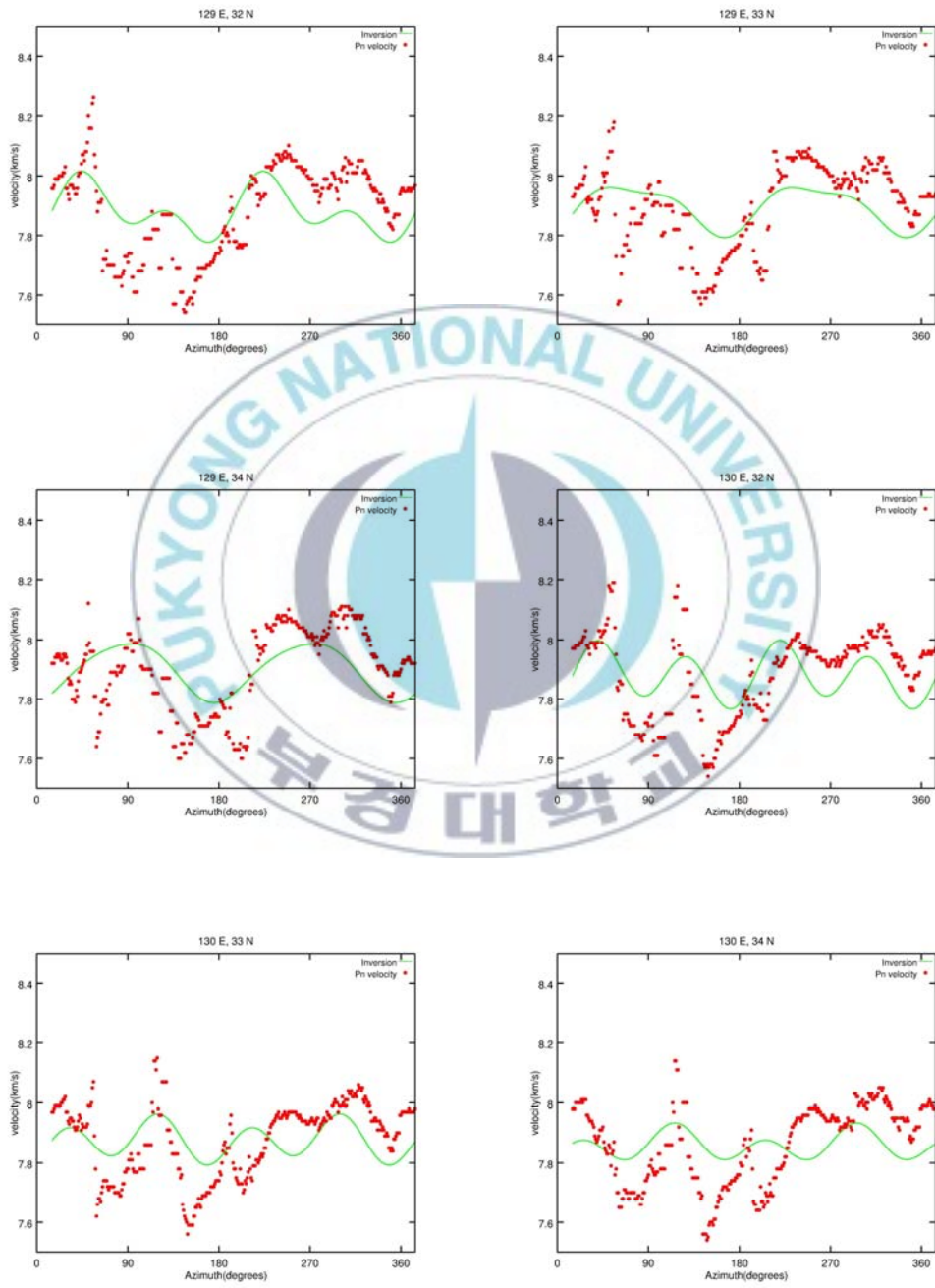
Latitude (°N)	Longitude (°E)	α_0	C	D	E	F	1 st fast direction		2 nd fast direction	
							ϕ	P_n	ϕ	P_n
32	130	7.8798	-0.0148	0.0320	-0.0802	0.0403	40	7.9979	126	7.8837
33	130	7.8751	-0.0246	-0.0130	-0.0370	0.0542	104	7.9272	120	7.9287
34	130	7.8590	-0.0175	-0.0227	-0.0107	0.0447	104	7.9162	116	7.9182
32	131	7.8716	-0.0043	0.0215	-0.0679	0.0467	37	7.9734	125	7.8563
33	131	7.8589	0.0019	0.0084	-0.0455	0.0497	33	7.9347	123	7.8374
34	131	7.8488	0.0049	0.0112	-0.0319	0.0184	37	7.8977	128	7.8488
35	131	7.8298	-0.0149	-0.0019	-0.0396	0.0106	44	7.8676	129	7.8829
32	132	7.8599	-0.0114	0.0429	-0.0507	0.0392	38	7.9620	122	7.8988
36	132	7.6599	-0.3812	0.1353	-0.3246	0.1233	48	8.1262	121	7.8694
32	133	7.9049	-0.0363	0.0427	-0.0364	0.0492	37	7.9929	115	7.9207
35	139	7.8645	0.0506	0.0064	-0.0344	0.0117	31	7.9228	194	7.9680
36	139	7.8561	0.0358	-0.0019	-0.0426	0.0151	35	7.9089	136	7.9791
37	139	7.8364	0.0303	0.0161	-0.0275	0.0247	31	7.9008	194	7.9574
39	139	7.8081	0.0262	0.0889	-0.0203	0.0454	31	7.9479	194	8.2353
36	140	7.8423	0.0483	0.0011	-0.0320	0.0213	29	7.9020	194	8.1991
37	140	7.8493	0.0527	0.0204	-0.0265	0.0498	26	7.9526	194	8.1282
38	140	7.8320	0.0496	0.0704	-0.0041	0.0523	25	7.9700	194	7.9970
39	140	7.8356	0.0203	0.0766	0.0001	0.0662	26	7.9726	194	7.8829
40	140	7.8375	-0.0030	0.0927	0.0531	0.0460	18	7.9497	194	7.8988
41	140	7.6983	0.2748	0.2097	-0.1514	-0.1625	47	8.0609	159	7.8694
33	141	7.8366	0.2051	-0.0299	0.0243	-0.1332	15	7.8960	164	7.9207
34	141	7.9087	0.0360	-0.0422	0.0005	0.0485	15	7.9609	120	7.9114
35	141	7.9012	0.0518	-0.0412	0.0076	0.0546	15	7.9765	192	7.9026

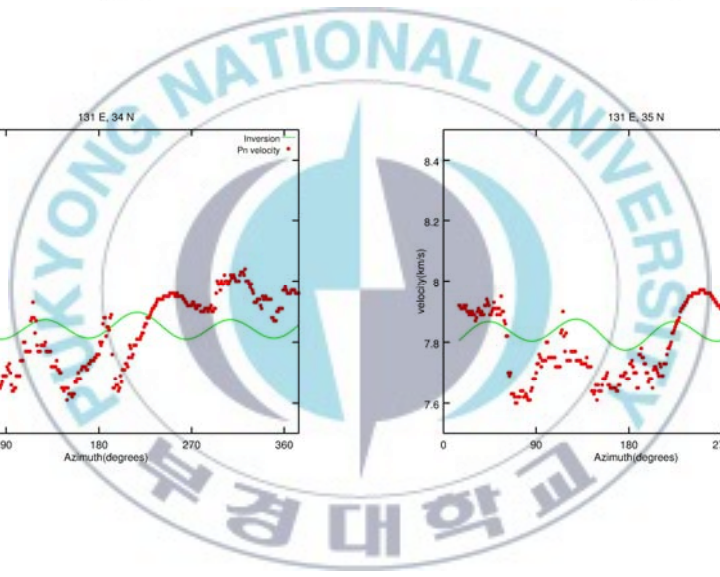
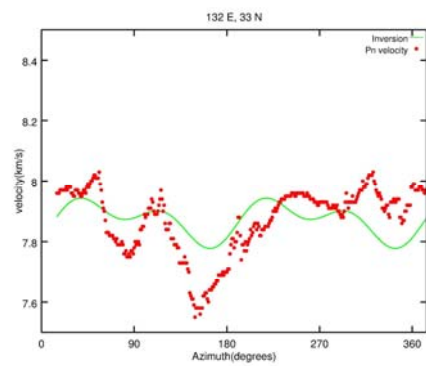
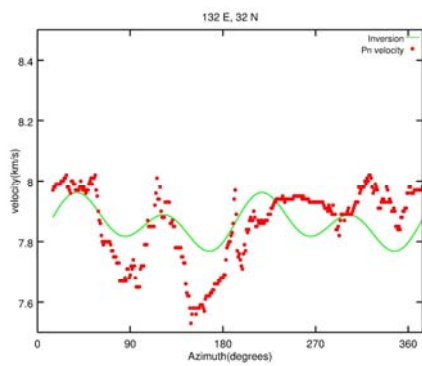
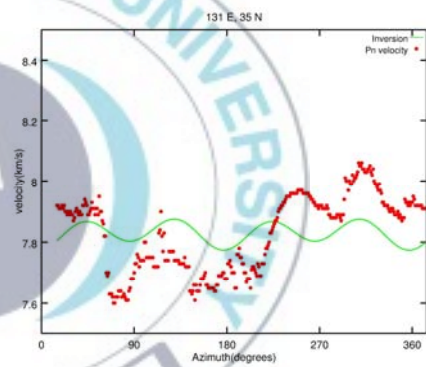
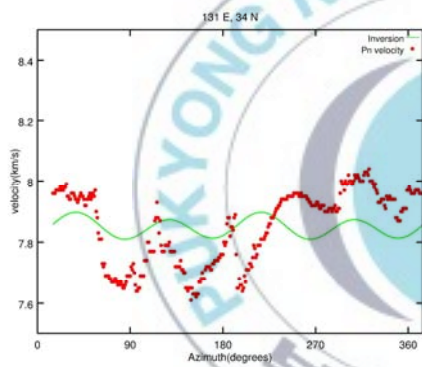
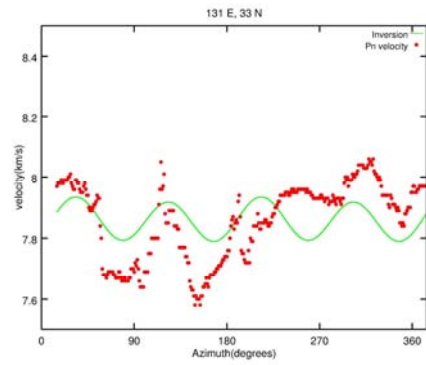
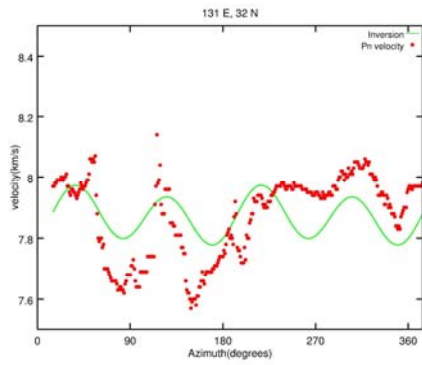
Latitude (°N)	Longitude (°E)	α_0	C	D	E	F	1 st fast direction		2 nd fast direction	
							ϕ	P_n	ϕ	P_n
36	141	7.8684	0.0211	-0.0286	-0.0229	0.0647	24	7.9281	121	7.9007
37	141	7.8857	0.0320	-0.0025	-0.0295	0.0836	25	7.9918	194	7.8759
38	141	7.8552	0.0338	0.0730	-0.0007	0.0591	25	7.9912	194	7.8853
39	141	7.8476	0.0068	0.0772	0.0227	0.0923	23	7.9993	194	7.8853
40	141	7.8471	-0.0257	0.1514	-0.0877	0.0155	80	7.9802	194	7.9319
35	142	7.9916	0.0524	-0.1556	-0.0548	0.1142	104	8.0824	125	7.9498
36	142	7.9504	0.0068	-0.1314	-0.0800	0.1031	104	8.0468	125	7.9444
37	142	7.9324	-0.0025	-0.0670	-0.0467	0.1303	104	8.0480	119	7.9462
38	142	7.8336	0.0340	0.0871	0.0307	0.0909	21	8.0107	194	7.9080

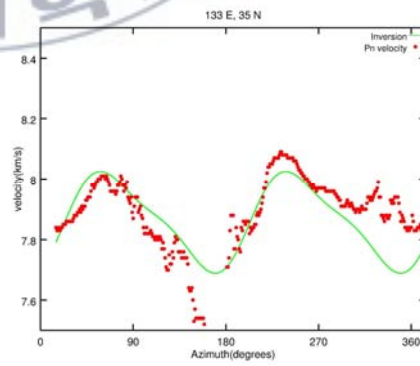
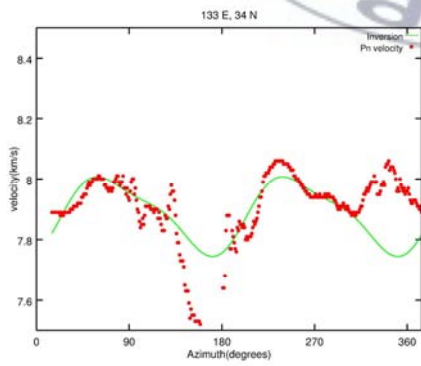
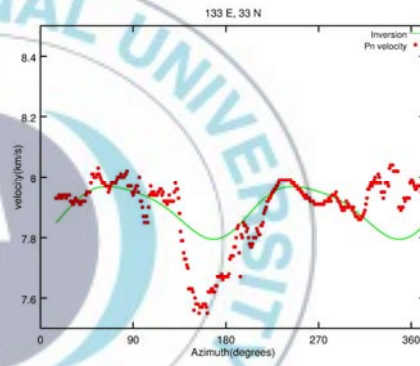
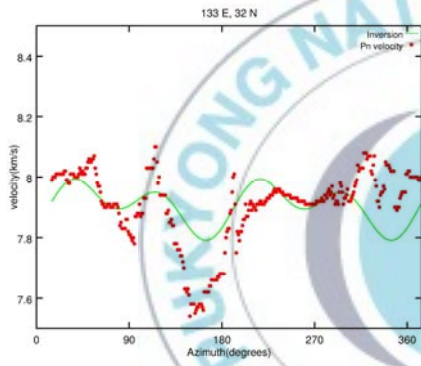
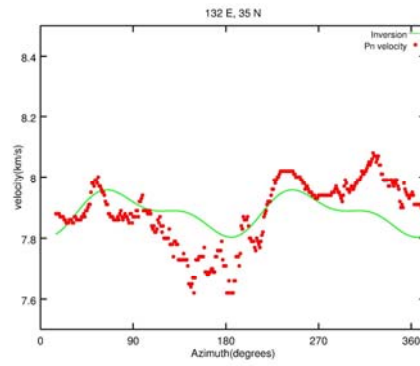
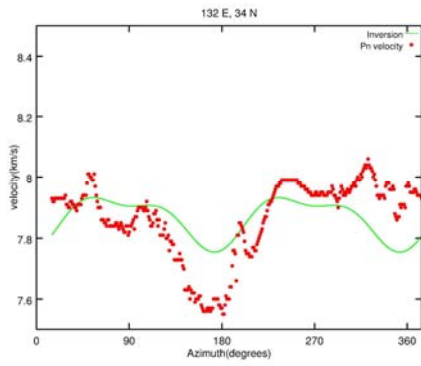


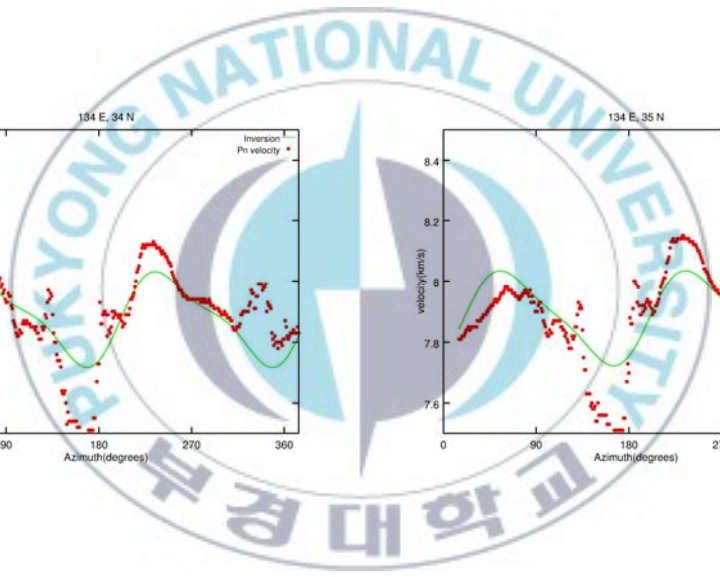
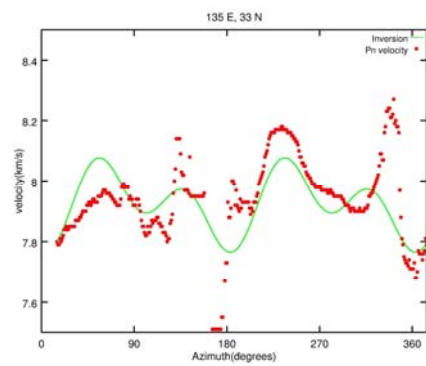
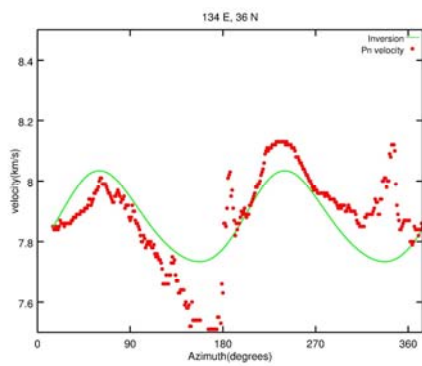
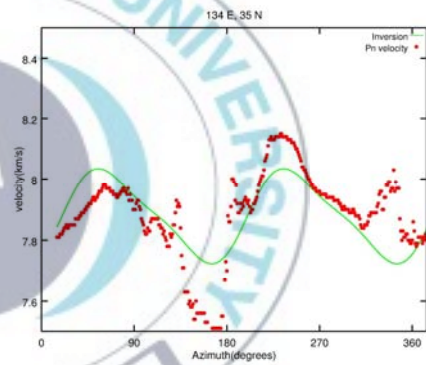
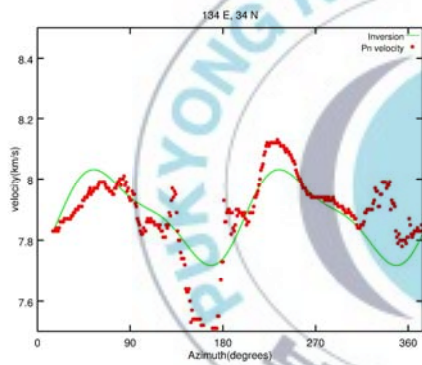
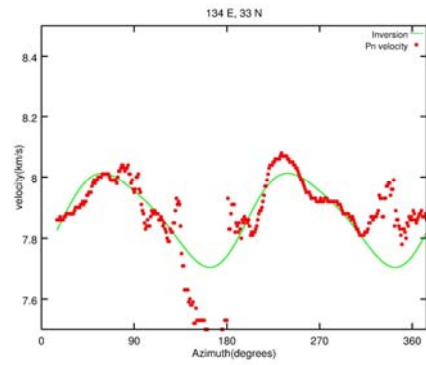
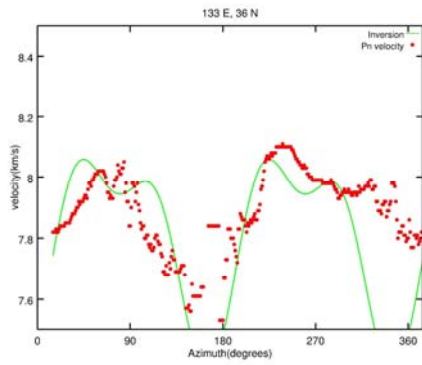
Appendix

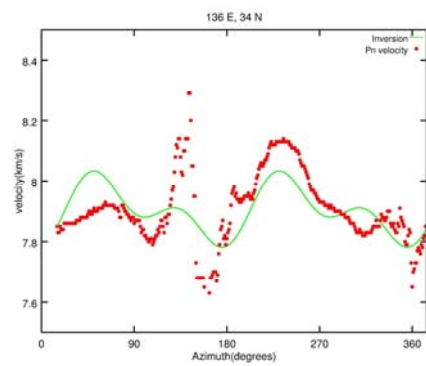
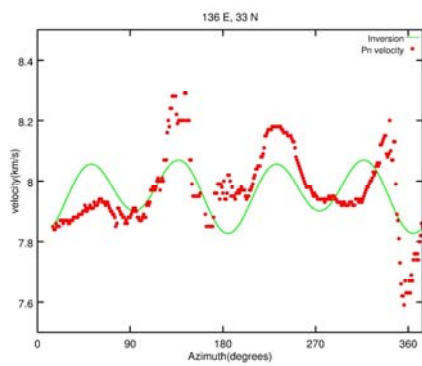
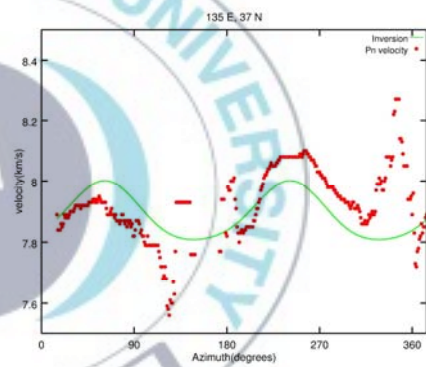
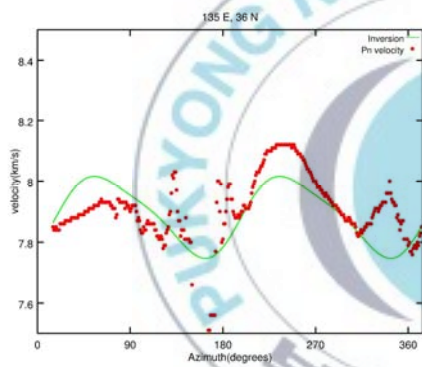
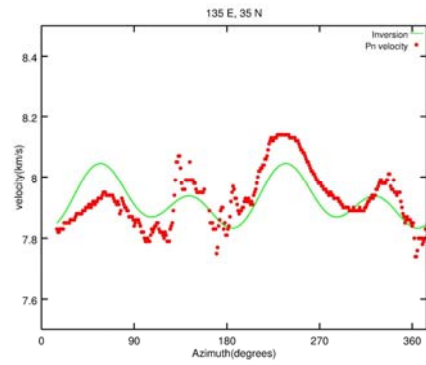
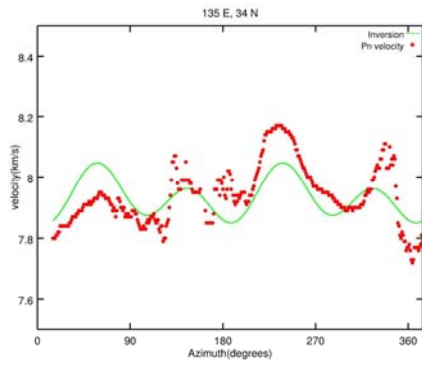
Supplemental Figures

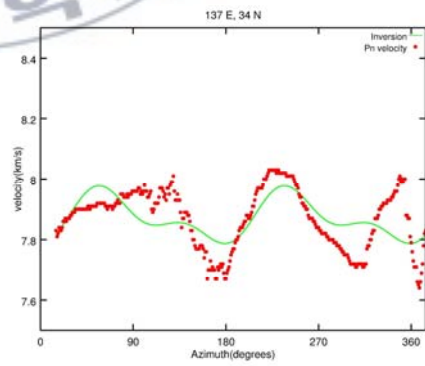
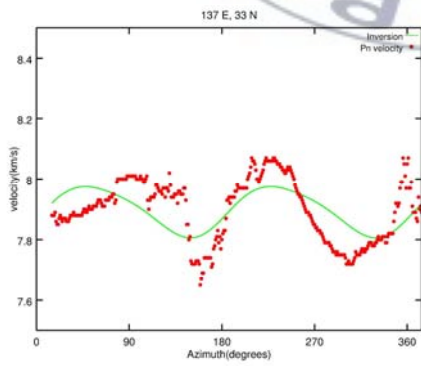
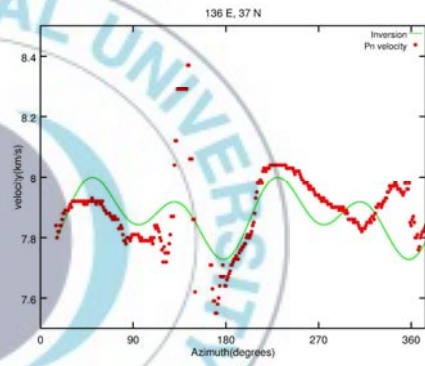
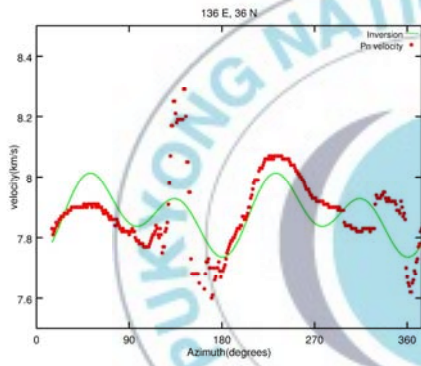
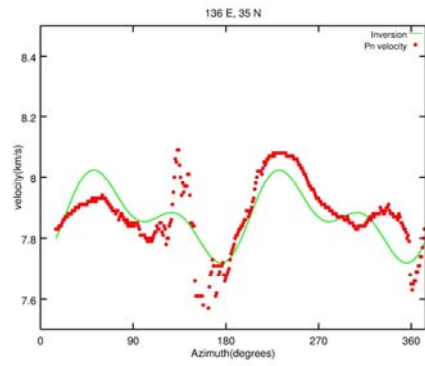
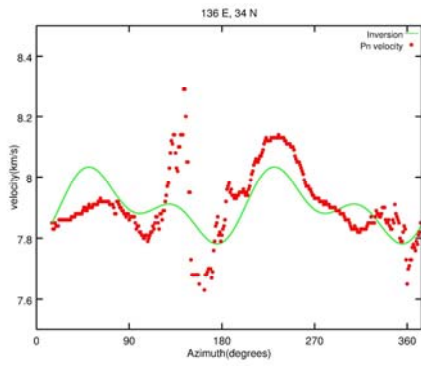


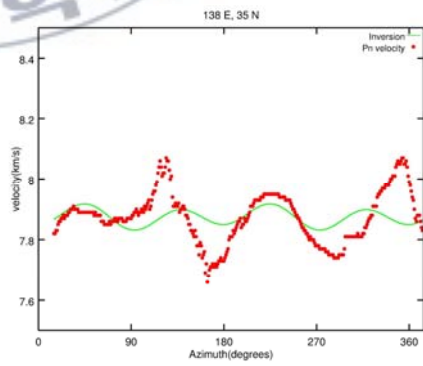
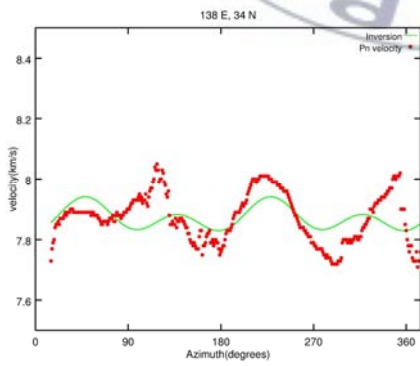
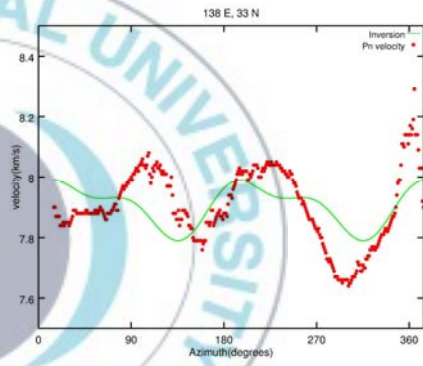
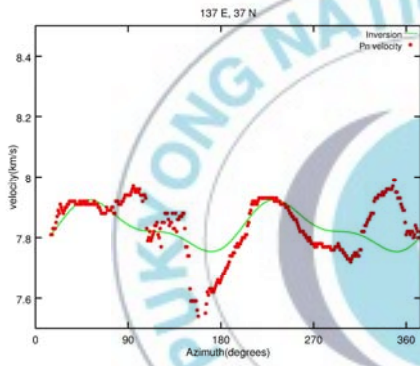
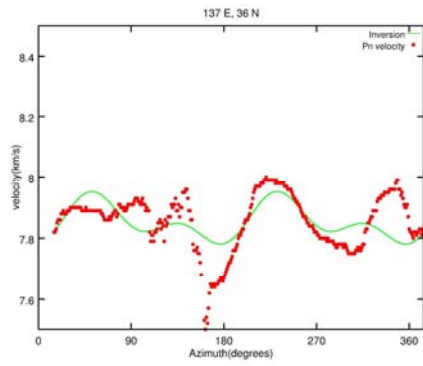
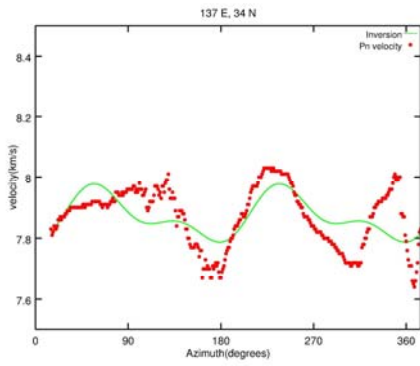


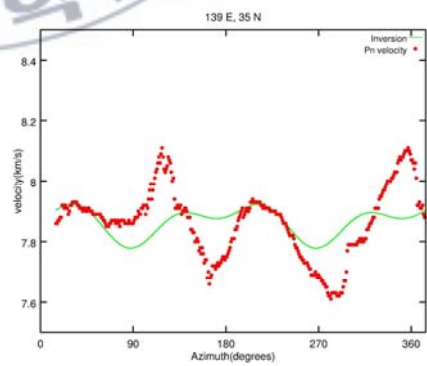
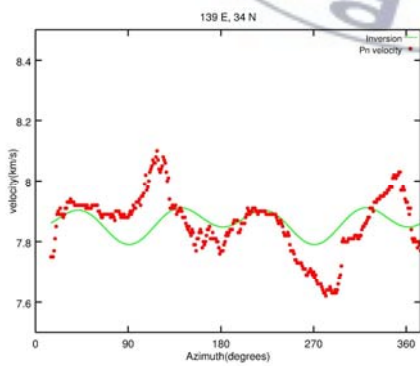
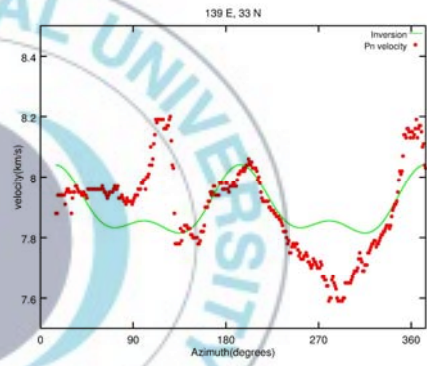
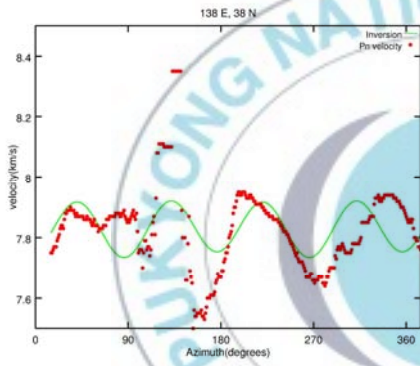
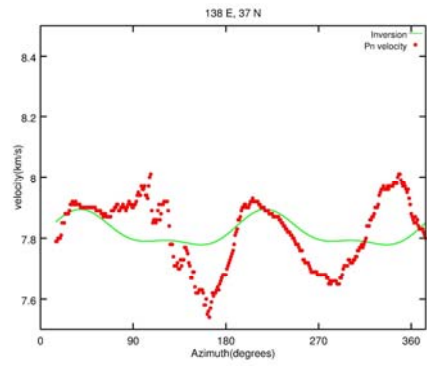
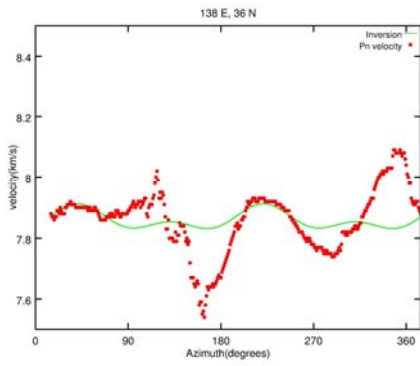


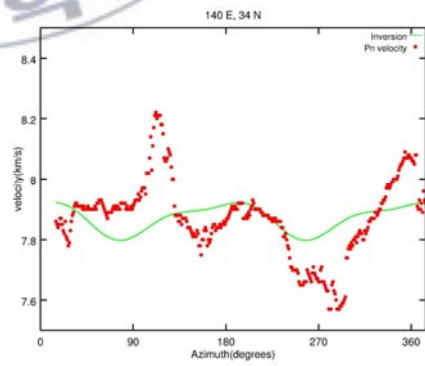
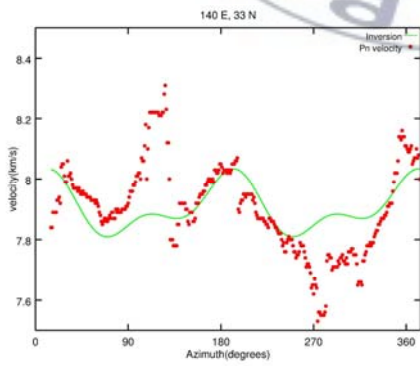
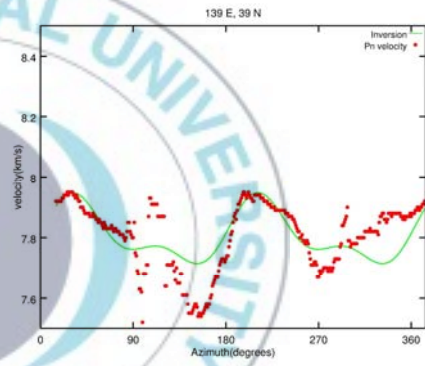
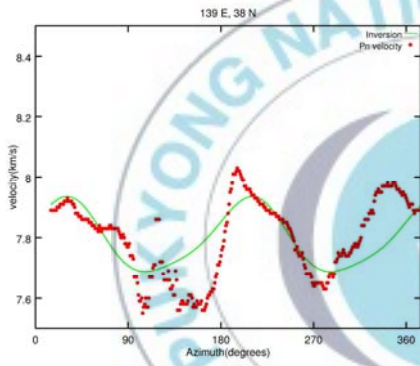
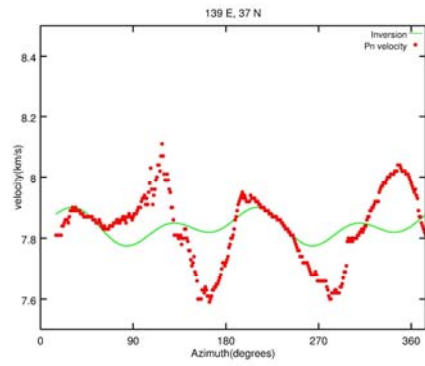
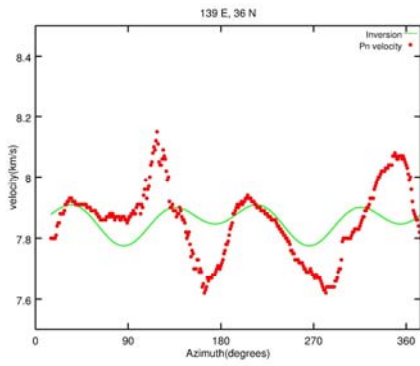


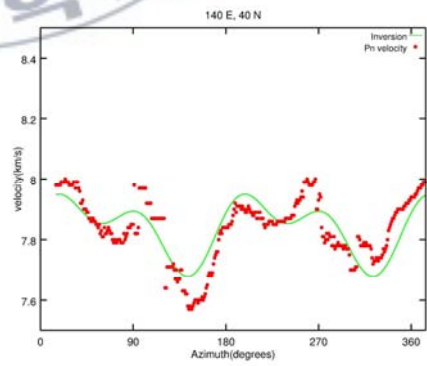
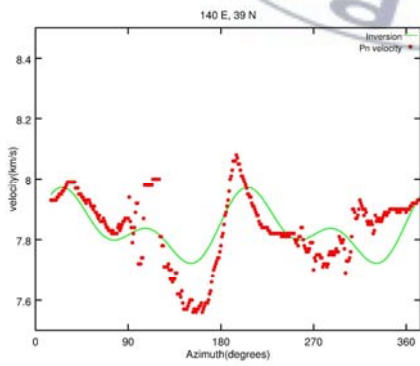
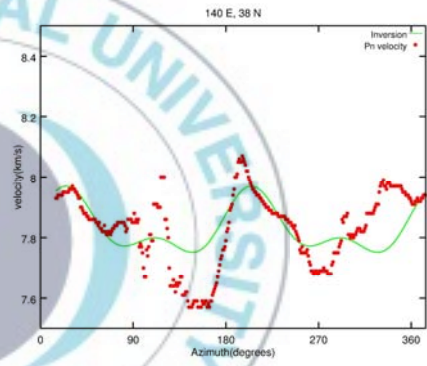
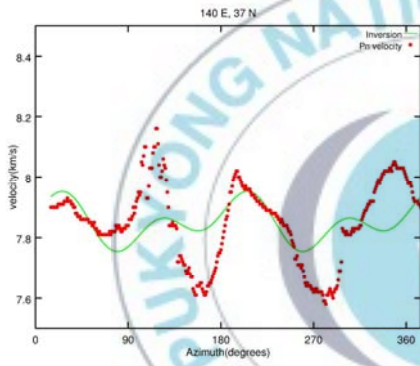
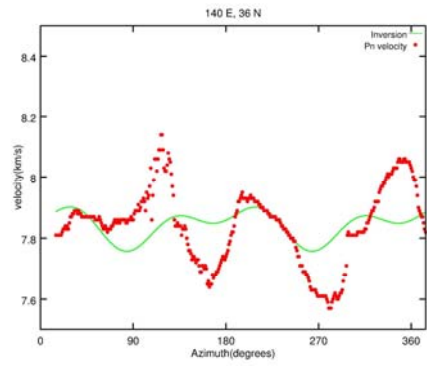
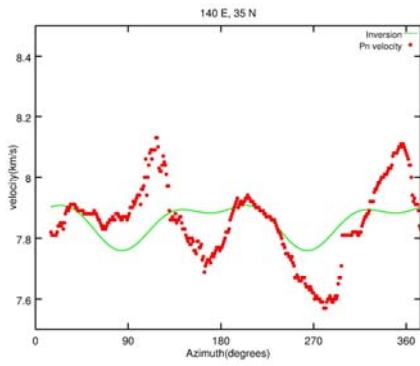


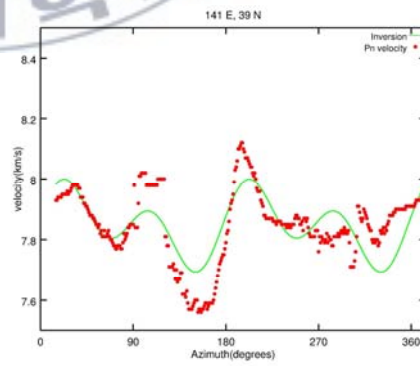
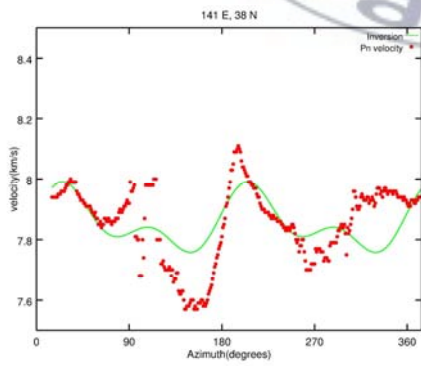
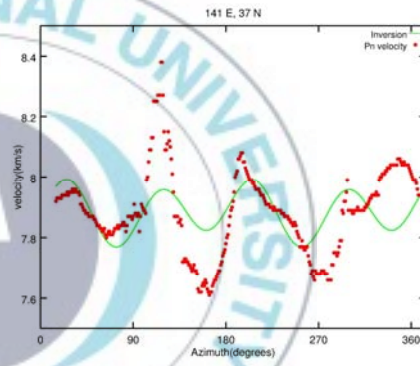
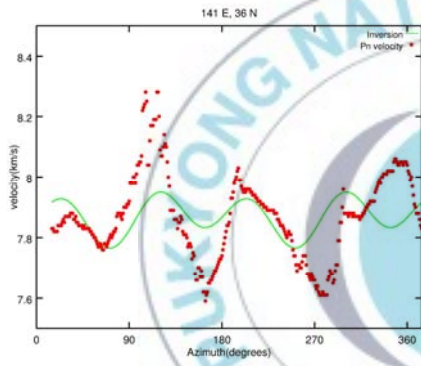
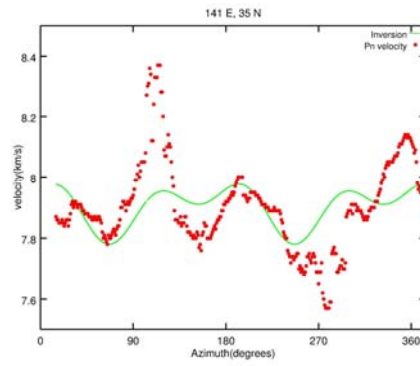
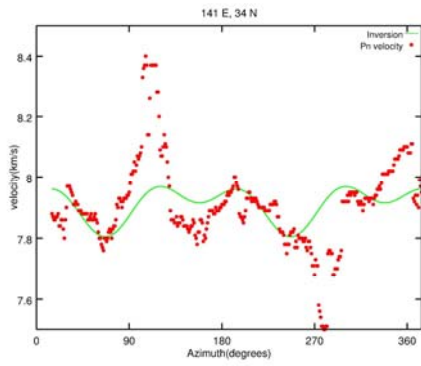


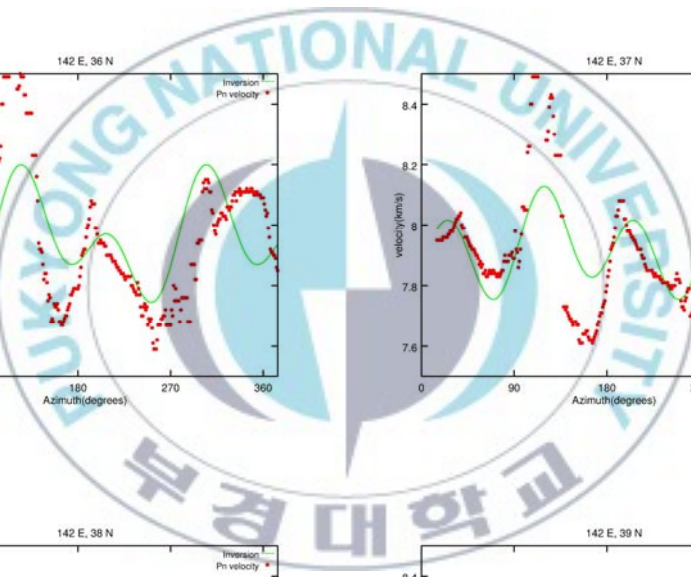
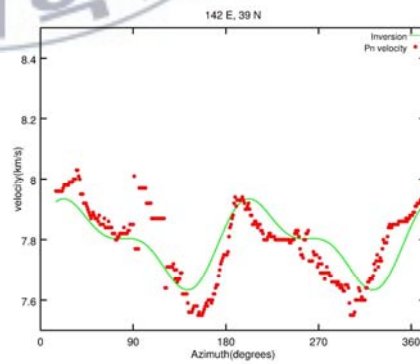
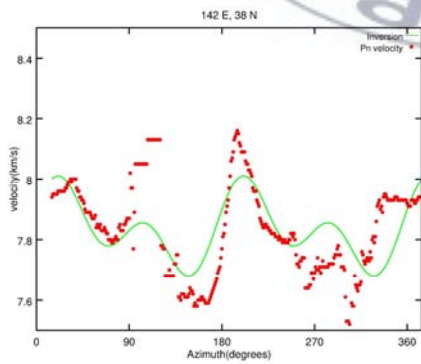
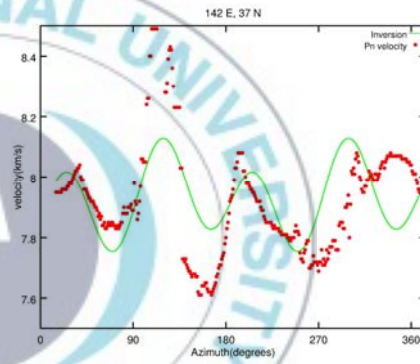
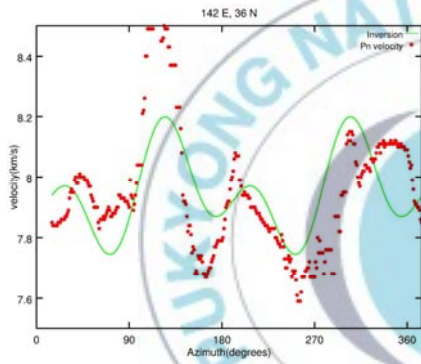
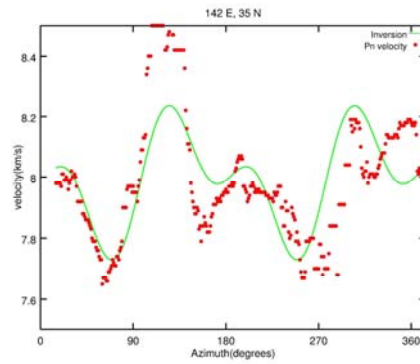
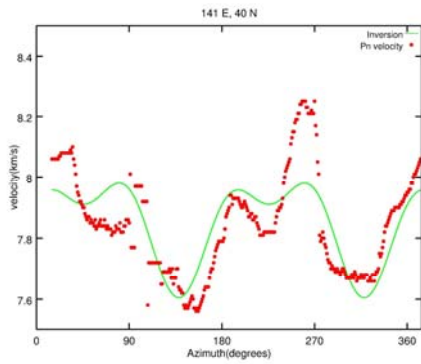


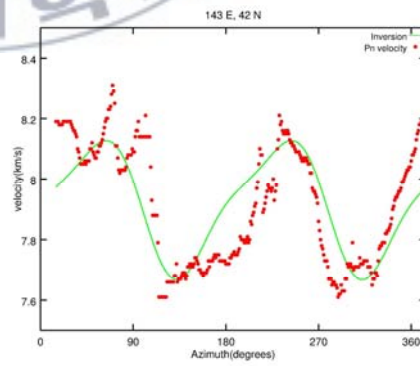
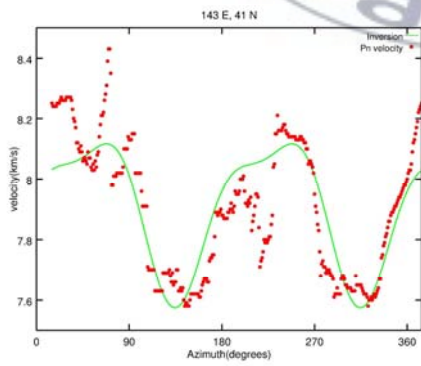
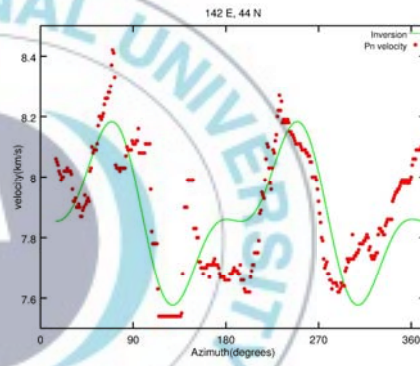
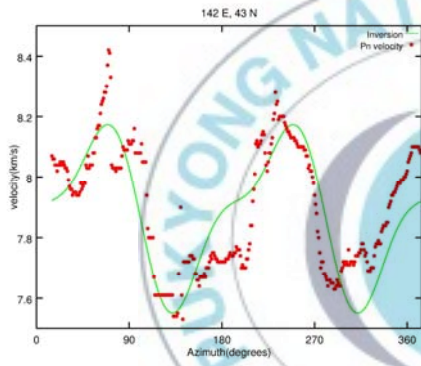
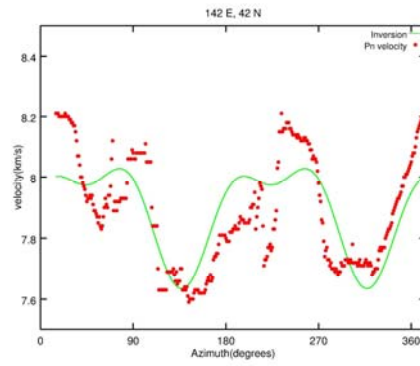
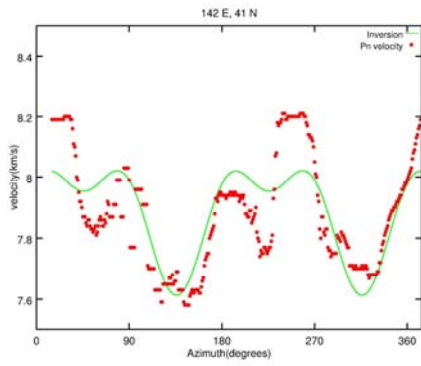


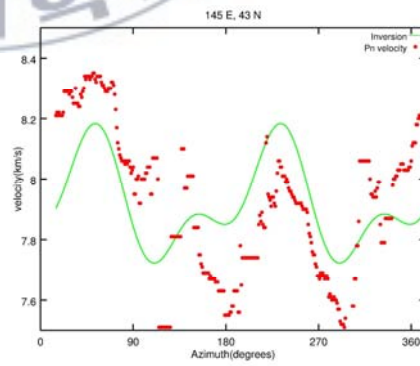
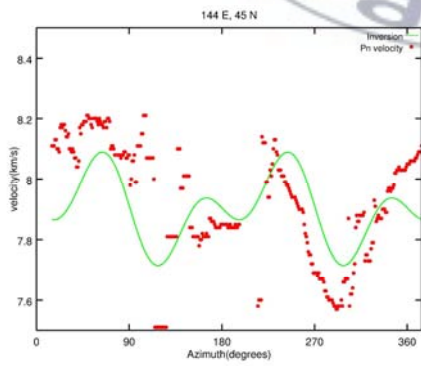
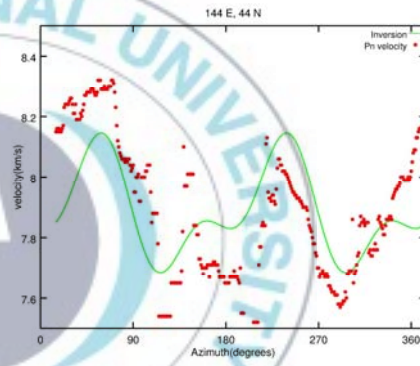
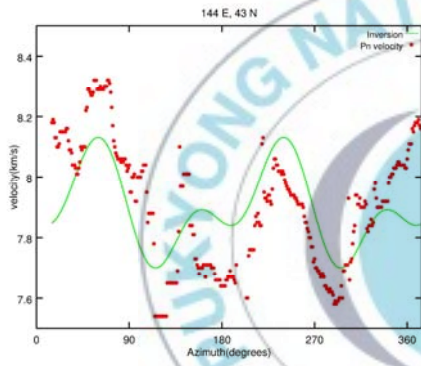
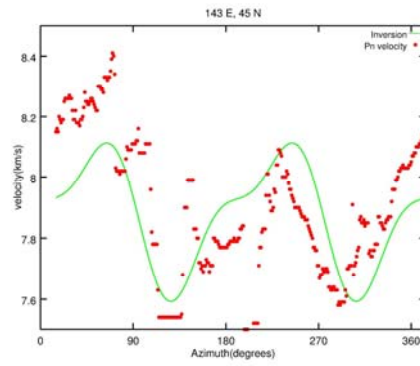
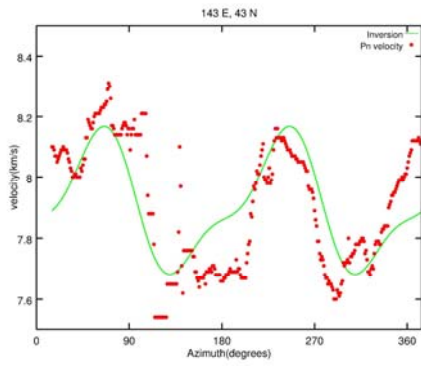


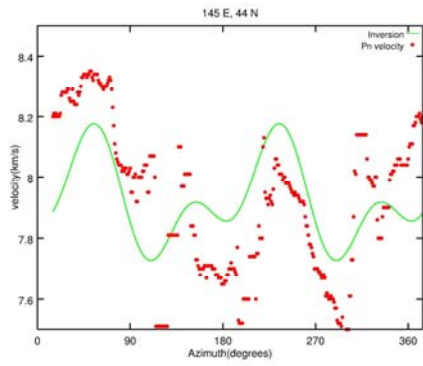












동아시아 지역 지진 P_n 파 이방성 연구

송 근 영

부 경 대 학 교 대 학 원 지 구 환 경 과 학 전 공

요 약

지진파의 이방성은 지구내부의 과거와 현재를 설명하는데 중요하다. 특정 방위 각에서 더 빠른 지진파 전파 속도를 확인하여 대륙 하부의 지진파 이방성 방향을 추정할 수 있다. 맨틀 최상부에서의 지진파 이방성을 확인하기 위하여 상부 맨틀과 지각의 경계면 사이인 mantle-lid를 지나는 P_n 파를 이용할 수 있다. ISC(International Seismological Centre)에서 1960년도부터 2011년까지 동아시아 지역의 진원 거리 1.5° 에서 15° 범위 내에서 발생한 모든 이벤트의 P_n 파 도착시간을 수집하였다. 지진계를 이용한 계기관측이 시작된 초기에 아날로그 지진계로 기록된 도착시간을 잘못 해석할 때 발생할 수 있는 시간오차를 제거하기 위해서 two-station method를 사용하여 P_n 파 전파속도를 추정하였다. 맨틀 최상부의 P_n 파 전파경로를 포함하는 이방성 지역에서는 방위각에 따라 P_n 파의 전파속도가 달라진다. 이 변화를 확인하기 위하여 동아시아 전역에 대하여 1° 간격의 격자를 구성하고, 격자 내부의 공간적인 범위에서 추정한 P_n 파 속도 분포로부터 지진 이방성을 추정하였다(Smith and Ekström, 1999). P_n 파 속도 및 분포를 이용하여 동아시아 지역의 P_n 파 속도에 대한 역산을 하였다. 이 연구를 통하여 얻은 P_n 파 이방성 분포와 역산결과로 동아시아 지역 상부 맨틀의 지진파 이방성을 확인하여 동아시아 지역에서 만나고 있는 판 경계 지역(섭입대 부근)에 대한 이방성이 일반적인 주기가 아닌 90° 의 주기를 가짐을 확인하였다. 특정 주기를 보이는 지역은 판구조활동에 의한 이방성의 결과나 다른 방향의 이방성 층을 지나가면서 영향을 받은 P_n 파가 두 방향으로 빠른 속도를 보이기 때문일 것이라고 예상가능하며 확인을 위한 연구가 계속 되어져야 할 것이다.